Flexible OPV modules for highly efficient indoor applications

Mari Ylikunnari[1], Marja Välimäki[1], Kaisa-Leena Väisänen[1], Thomas M. Kraft[1], Rafal Sliz[2], Gianni Corso[3], Marja Vilkman[4]

[1] VTT Technical Research Centre of Finland, Kaitoväylä 1, FI-90571 Oulu, Finland
[2] University of Oulu, Optoelectronics and measurement techniques laboratory, 90014 University of Oulu, Finland
[3] Eni S.p.A, Renewable Energy & Environmental R&D, Via Fauser 4, 28100 Novara, Italy
[4] VTT Technical Research Centre of Finland, Tietotie 3, FI-02150 Espoo, Finland

E-mail: mari.ylikunnari@vtt.fi

Abstract

The comparison of solution processed organic photovoltaics (OPVs) with two roll-to-roll coated electron transport layers (ETL), as well as printed grid or solid back electrodes provides insight into the future of R2R fabricated architectures. The variation in performance of the R2R slot-die coated zinc oxide (ZnO) versus the tin oxide (SnO_2), showed a clear dependence on the spectrum of the illumination source. It was found that under indoor light conditions (200 - 1000 lux LED and fluorescent sources) the SnO_2 outperformed the ZnO with highest efficiencies near 13 % and 10 % respectively. This is in contrast to results obtained under 1 sun (AM 1.5) in which the cells fabricated with a ZnO ETL had a higher power conversion efficiency than those prepared with SnO_2. The results also confirm the significance of the layout of the printed silver back contact; in which cells with the grid structure outperformed those with full coverage by approximately 35 % for ZnO and just under 10 % for SnO_2 (all light conditions). The combination of a R2R coating and S2S printing process to prepare modules with 8 cells in series (PET/ITO/SnO_2/PV2001:PCBM/PEDOT:PSS/silver grid) resulted in a PCE of 13.4 % under indoor office light conditions.

Keywords: Organic photovoltaics, indoor light, R2R, S2S, Polymer solar cells, Solution-processed

Introduction

Light sources that are accessible to everyone, and everywhere are lacking full-scale utilization. Solar energy technologies are able to provide solutions for Internet-of-Things (IoT) based applications such as smart gadgets, as well as intergrating them into buildings for the purpose of harvesting energy in the form of smart walls/surfaces. **[1] [2]** None of the existing thin-film technologies have yet reached the efficiency levels and lifetimes of traditional silicon PV systems, but they have the huge potential to spread into a wide range of end-use areas due to the lightweight and flexibility. **[3]** In addition, the capability of using well-established and widely used roll-to-roll (R2R) mass-production methods under ambient atmosphere, and utilizing materials that are toxic-free is an advantage obtained with organic photovoltaics (OPV). **[4] [5]**

The ability to obtain high power conversion efficiencies (PCE) under different lighting conditions is one of the main benefits of using OPVs. [1] Until now, over 17% record efficiency for OPV cells under solar irradiation has been obtained. [6] [7] Polymer-based donor-materials has reached PCE of over 16% with ternary bulk-heterojuction (BHJ) structure and also by using non-fullerence ternary BHJ structure, respectively. [8] [9] So far, the highest 28.1% efficiency under indoor light for OPV has been obtained with small molecule-based cells. Likewise, the efficiencies obtained with polymer-based cells have reached 26.1% with a ternary structure and 18.72% with a binary structure. [10] [11]

Until now, indoor characterization of polymer-based OPV have covered poly(3-hexylthiophene) (P3HT), poly[(2,5-bis(2-hexyldecyloxy)phenylene)-alt-(5,6-difluoro-4,7-di(thiophen-2-yl)benzo[c][1,2,5]thiadiazole)] (PPDT2FBT), thieno[3,4-b]thiophene-alt-benzodithiophene copolymer (PTB7), poly([2,6′-4,8-di(5-ethylhexylthienyl)benzo [1,2-b,3,3-b]dithiophene]3-fluoro-2[(2-ethylhexyl)carbonyl]thieno [3,4-b]thiophenediyl) (PTB7-Th), poly[N-9″-heptadecanyl-2,7-carbazole-alt-5,5-(4′,7′-di-2-thienyl-2′,1′,3′-benzothiadiazole)] (PCDTBT). [1] [11] [12] [13] [14] [15] [16] [17] [18] There have however been few studies that have dealt with processing on PET substrate instead of glass, and fabrication of the actual modules. [17] [19] Among other donor-polymers, the solution processable PV2000 with [6,6]-phenyl C61 butyric acid methyl ester (PCBM) has shown PCE of 4.3 % and 8.0 % with fully ink-jet printed and spin-coated devices under solar irradiation, respectively. [20] [21] [22] Quite recently, the PCE of PV2000-based material have reached 7.56 % in solution-processed modules prepared in ambient conditions with the possibility to operate in a wide range of film thickness. [23]

From solution processable materials, polyethylenimine (PEIE), poly [(9,9-bis(3′-(N,N-dimethylamino)propyl)-2,7-fluorene)-alt-2,7-(9,9-dioctylfluorene)] (PFN), titanium oxide (TiO$_x$) and zinc oxide (ZnO) have been used as electron transport layer (ETL) under indoor light conditions. [1] [12] [14] [15] [17] However, ZnO is dependent on light soaking. Thus, it might not be the most optimal ETL material for low light intensities. [24] Only a few studies have addressed the use of solution processed hole transporting and hole conctact materials for indoor OPV by using poly(3,4-ethylenedioxythiophene) polystyrene sulfonate (PEDOT:PSS) with silver or carbon paste. [25]

Currently, studies to replace the ZnO with tin oxide (SnO$_2$) for indoor light conditions to avoid additional light soaking have not been reported. Furthermore, research related to the indoor evaluation of PV2000-based cells appear to be nonexistent, eventhough the possibility of obtaining higher thickness could prevent leakage current, thus being more suitable for the cells to operate under indoor light. [23] [15]

Herein, OPVs were prepared by R2R slot-die coating and screen printing on a flexible plastic substrate indium tin oxide (ITO)-PET/ZnO/PV2001:PCBM/PEDOT:PSS/silver and ITO-PET/SnO$_2$/PV2001:PCBM/PEDOT:PSS/silver cells and modules see **Figure 1**. Hole contact was printed as a full active area coverage and as a honeycomb-patterned grid. The use of honeycomb-structured as hole conctact was considered to provide sufficient conductivity for low light intensities. Electrical characterization was performed using solar irration, fluorescent light and LED light at different intensities to verify the spectral compatibility indoor light sources as well as the absorption of thick PV2001:PCBM. SnO$_2$ was preferred as an ETL instead of ZnO in indoor illumination together with a grid-patterned silver electrode. The average PCE in the modules were measured under fluorescent lamp (FL) with silver as a grid and SnO$_2$ as the ETL.

Methods

In this study, a series of printed and coated organic solar cells were prepared comprising two electron transport material and two top electrode patterns. All cells were prosessed on patterned (50 Ω/□) ITO coated PET foil with a thickness of 125 µm. ETL layer consisting of ZnO or SnO$_2$ was slot-die coated with a roll-to-roll (R2R) pilot printing machine. ZnO (N-12) and SnO$_2$ (N-31) nanoparticle solutions in alcohol were purchased separately from Avantama. A blend of PV2001 and PCBM with a mass ration of 1:1,5 in o-xylene was coated with the same technique. PV2001 was purchased from Raynergy Tek and PCBM from Nano-C. At this point, the substrate was cut into sheets and processed as sheet-to-sheet (S2S). Flat bed screen printing was used to print the hole transport layer (HTL) followed by the top electrode. The silver electrode had full coverage or a honeycomb pattern. HTL ink was PEDOT:PSS aqueous solution from Agfa (EL-P5015) and silver ink (XPVS-670) was purchased from PPG Industries. The devices were prepared in ambient environment and stored under nitrogen atmosphere in between processes. Finally, devices were encapsulated with 3M FTB3-50 barrier and pressure sensitive adhesive from Adhesives Research.

Current-voltage (I-V) characterization was performed with an AM1.5G solar simulator (Atlas Solar Cell Test 1200) calibrated to 100 mW cm^{-2} using a calibrated Si-reference cell filtered with a KG5 filter. Indoor light measurements were carried out with two light sources, fluorescent light (Osram L18W/830) and LED light source (Nichia_3800K.int) in four illuminance level of 200, 400, 800 and 1000 lux. The lux level was adjusted by changing the distance between a light source and a sample holder. The illuminance value (lux) and light source spectrum togerher with light power spectrum (mW cm^{-2}) were measured with Konica Minolta Illuminance Spectrophotometer CL-500A. Power spectrum was measured for both light sources at each lux level and the irradiance was calculated by integrating the individual spectrum. Totally 16 cells from each sample group were taken into AM1.5 measurements with an active area of 33 mm^2 together with three modules of ZnO and SnO$_2$ that had a grid structure in the top electrode and an active area of 1360 mm^2. Modules comprised 8 serially connected cells. UV-vis and transmission spectrums were obtained using Varian Cary 5000 UV-vis-NIR spectrophotometer. The External Quantum Efficiency (EQE) measurements were performed using Automated Spectroradiometric Measurement System - Optronic Laboratories (USA). The spectral response of the solar cells was measured at a wavelength range of 300 – 900 nm with resolution 10 nm. The light beam size was limited to 1 mm in diameter. To avoid sensor saturation, the light beam was chopped at a 167 Hz using an integrated lock-in amplifier. The sample cells were connected to the measurement system through the microprobe measurement system. After the measurements, the acquired data together with the QE energy conversion factor were used to calculate the EQE.

Results and Discussion

Spectra of light sources

Majority of OPV measurements are done under sunlight conditions such as AM1.5G measurements. However, the performance in these conditions does not reveal the behaviour of OPV in indoor lighting. [26] There are no standardized method to evaluate the indoor performance of solar cells but a large group consensus recommends FLs with an illuminance level between 200 – 1000 lux, which corresponds to normal office light level. [27] Another widely used light source is LED that has spread into home and offices due to its low power consumption and much broader light spectrum than a FL as seen in Figure 2. A significant portion of these indoor light spectra are in the 600 nm range. A polymer that has good absoption spectral compatibility with indoor light sources is expected to be suitable for indoor applications. [16] The spectral match indicates that under indoor lighting the PCE of OPV is expected to be higher than under sunlight, because a cosiderable part of the sunlight spectrum is within the infrared region. The PCE is determined as the ratio of the solar cell maximum output power to the incident power on the solar cell from the lighting source. Since the spectrum of FL and LED light are different, irradiance (mW/cm^2 unit) was calculated by integrating the spectrum of individual lux level in order to determine the PCE (Supplementary Fig. 1). The same lux level of FL and LED resulted in different light intensity as seen in Table 1.

Material properties

Among various materials, metal oxides in particular have attracted a considerable attention as electron transport and hole blocking material in organic solar cells. TiO$_x$ and ZnO are mostly used due to their optical transparency, high electron mobility, good stability and processability. [28] [29] [30] In order to effectively utilize these metal oxide materials in the ETL, systems with a double ETL have been introduced where ZnO is combined with an additional layer of SnO$_2$, Al-doped ZnO or conjugated polymer to improve the interfacial properties and photovoltaic parameters. [31] [32] [33] [34] Recently, SnO$_2$ has emerged as a promising ETL material to replace ZnO or TiO$_x$. ZnO has photocatalytical activity under UV light and both materials require a well-known light soaking to improve the performance level of organic solar cells. [35] [36] So far SnO$_2$ has been widely used as an ETL for high performance perovskite solar cells. [37] [38] [39] [40] SnO$_2$ is a light-soaking-free material due to its wider band gap as compared to ZnO and SnO$_2$ nanoparticle has proven to be suitable for solution processing. [41] [24] [42] [43] It is therefore a suitable alternative for complete solution processed roll-to-roll OPV comprising printing or slot die coating.

The UV–light absoption of ZnO is seen in Figure 3 together with the optical transmittance spectra of our slot die coated ZnO and SnO$_2$ on PET substrate. At 380 nm, the transmittance drops to 50% in ZnO whereas the decrease in transmittance of SnO$_2$ is at 330 nm. Both SnO$_2$ and ZnO nanoparticle layers have a good transmittance around 90 % between 500 – 800 nm. This is an ideal range to harvest indoor light from FL and LED that have most of the light intensity in the same region (see Figure 2). In addition, the absorption spectra of PV2001:PCBM blend shown in Figure 4 has a broad absorption between 530 – 750 nm, thus has a good spectral overlap with that of the FL and LED.

Indoor light requires an active material with high open-circuit voltage (V_{OC}) in 1 sun. V_{OC} has a logarithmic dependence on the photocurrent density, which in turn is approximately linearly proportional to the incident light intensity. [1] [16] As the light intensity decreases under indoor lighting OPV devices with high V_{OC} under 1 sun are expected to have a fairly good V_{OC} also in indoor applications. The enhancement of photocurrent in OPV devices under indoor lighting is closely related to the maximum light absorption and minimum leakage current. [17] To minimise the leakage current trough pinholes and to allow more photons to be absorbed, a thicker active layer is more suitable for indoor systems in comparison to an outdoor system at 1 sun. [15] As a result, the OPVs produced in this study for indoor lighting have a comparatively thick photoactive layer (PAL) (600 nm in cells and 800 nm in modules) and exhibit high V_{OC} under 1 sun condition. Both the cells and modules with the active blend of PV2001:PCBM give an average V_{OC} of 0.75 V/cell in 1 sun regardles which ETL material was used (see Table 2).

Illumination under 1sun and indoor light

Before comparing the OPV performance under low light, the performance under 1 sun condition was first studied and the results are shown in Table 2. In AM1.5 measurements, the ZnO with a grid structure in top electrode (ZnO/grid) had the highest average PCE of 4,4 % in cells. This resulted in slightly higher current in comparison to SnO_2/grid containing cells, which had an average PCE of 3.9 %. Consequently, the maximum output power (P_{mpp}) of ZnO/grid cells was the highest, providing 1.5 mW whereas 1.3 mW was obtained with SnO_2/grid. Since there was no significant difference in AM1.5 measurement between the top electrode patterns (full coverage vs. grid), 1 sun measurements were conducted for module comprising 8 serially connected cells with grid structure in top silver electrode, see . The encapsulated modules generated PCE of 4.6 % and 3.4 % for ZnO and SnO_2 containing devices, respectively. In upscaling of OPV cells to modules the performance remained nearly the same. Only the average current density per cell (J_{SC}/cell) increased for ZnO modules from 11.87 to 14.35 mA/cm^2 and decreased for SnO_2 modules from 11.76 to 10.10 mA/cm^2, but V_{OC} remained at 0.75 V/cell and FF was between 0.4-0.5. Changes in J_{SC} refers to light absortion efficiency (changes in the layer thickness of PAL) and also to fluctuation in interfacial charge transfer efficiency due to delamination, degradation of materials or trap formation, which also affect the FF and serial resistance. [15] [44] The calculated average serial resistance (R_S) from the I-V curve of modules under AM1.5 illumination are shown in Table 4. R_S was 56.6 Ω and 45.9 Ω in ZnO and SnO_2 containing modules, respectively, suggesting that ZnO modules were inferior to SnO_2 modules in terms of charge transport trough PAL/ETL interface.

For indoor lighting measuremets three best working cells in AM1.5. were taken from each group and measured under 200, 400, 800 and 1000 lux for FL and LED. Measuring parameters are listed in Table 3. The difference in photovoltaic behavior between ZnO and SnO_2 devices was more distinct under indoor light conditions where devices containing SnO_2 as ETL were performing better than devices with ZnO. PCE in the cells were between 5.6-10.0 % and 11.4-13.5 %, while PCE in modules were 9.0-10.8 % and 12.3-13.4 % for ZnO and SnO_2 devices, respectively, regardless wether the indoor light source was FL or LED. The diffenrence between ZnO and SnO_2 is more clearly seen in EQE measurement of OPV cells shown in Figure 4 where SnO_2/grid exhibited much higher EQE of 76.2% than ZnO/grid cells with EQE of 57.5%. Most likely this is due to the fact that UV-light exposure of ZnO was needed for device activation process, thereby to decrease the charge extraction barrier of ZnO layer in AM1.5 measurement. [5] [23] Fluorescent lamp and LED light lack the UV-light portion that is shown as a red circle in AM1.5 spectrum in Figure 2.

In addition to ETL material, grid structure in top electrode resulted in much higher PCE values for cells than for full coverage top electrode. The superiority of the grid structure was more evident in ZnO cells as compared to SnO_2 cells due to the slightly greater I_{SC}/J_{SC} and FF values of ZnO/grid devices in comparison to ZnO/full. A significant enhancement of FF from AM1.5 measurements was observed especially in SnO_2/grid cells showing an increment from 44 % up to 67 % under FL/LED, which is an indication of good charge transfer between PAL and ETL/HTL. [44] As a result, the highest PCE of 13.5 % in cells was obtained from SnO_2/grid under 400 and 800 lux FL.

The current values I_{SC}/J_{SC} and P_{max} parameteres under the LED light were sligtly higher than under FL as the input power intensity was higer for LED than FL at each illuminance value. However, this was taken into account in PCE and the difference evened out mostly and at some illuminance the FL gave higher PCE than LED. The I_{SC}/J_{SC} increased along with the illuminance level as well as V_{OC}, and at 1000 lux the V_{OC} reached the level of 0.6 V in each cell type. A similar kind of trend in I_{SC}, J_{SC}, P_{max}, V_{OC} and PCE as a function of illuminance and light source type was obtained for the modules. Under 200, 800 and 1000 lux FL, the SnO_2/grid modules showed an average PCE of 13.4 %, which was the highest PCE obtained from modules in this study under indoor lighting. This is the highest reported indoor efficiency for R2R upscaled, fully solution processed modules
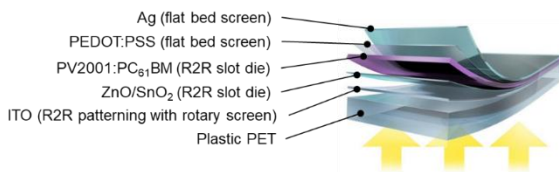
prepared on flexible substrate. In 1 sun illumination a series resistance is the limiting factor to the performance of OPV especially for the FF and J_{SC}, whereas low light intensity requires a high shunt resistance (R_{SH}) to prevent leakage current in the device since the photoinduces current density is low. [17] [45] The averege R_{SH} was more than 1.5 times greater in SnO_2 than ZnO modules. Table 4 validates the excellence of SnO_2 as ETL in OPV devices expanded to indoor light.

Conclusions

The performance of a fully solution processed inverted OPV devices on a flexible substrate under 1 sun as well as under different indoor light sources and illuminance conditions was studied. A comparison between two electron transport materials ZnO and SnO_2 and two back electrode pattern was made. The transmittance of electron transport layers and spectral overlap between the spectra of the different indoor light sources, as well as the absorption of PV2000 donor polymer was a good match for producing relativlely high efficient devices under fluorescent lamp and LED illumination. At a certain lux level, LED has a higher irradiance (mW/cm^2) than a FL, and that was observed as an increment in current values. The increased current values was also observed in grid structured top electrode cells from fully covered alongside to slightly increased V_{OC} and FF. The encapsulated SnO_2 containing samples with grid structured top electrode demonstrated high indoor light harvesting properties with power conversion efficiency up to 13.5 % in cells and 13.4 % in modules. The devices exhibit a stable PCE from cells to modules under indoor light both in ZnO and SnO_2 containing devices. The good performance of light soaking free SnO_2 nanoparticle ink was shown to be an alternative material for ZnO nanoparticle ink when used as an electron transport material in solution processed OPV devices for indoor applications.

Acknowledgements

(a)

(b)

Figure 1 (a) Schematic representation of the OPV devices and (b) photograph of modules and cells in this study
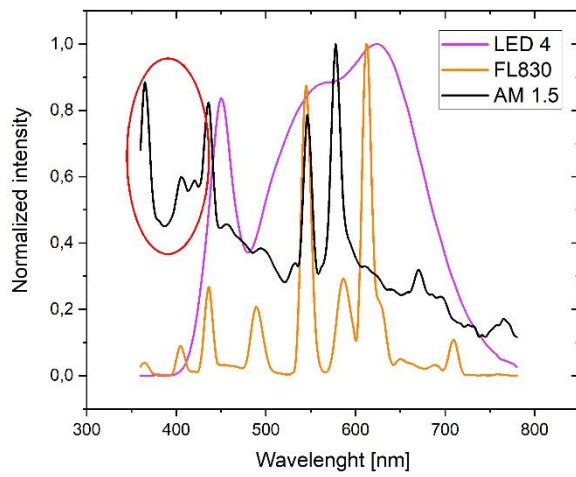

Figure 2 Normalised emission spectrums of AM1.5 solar simulator and indoor light sources at 1000 lux.
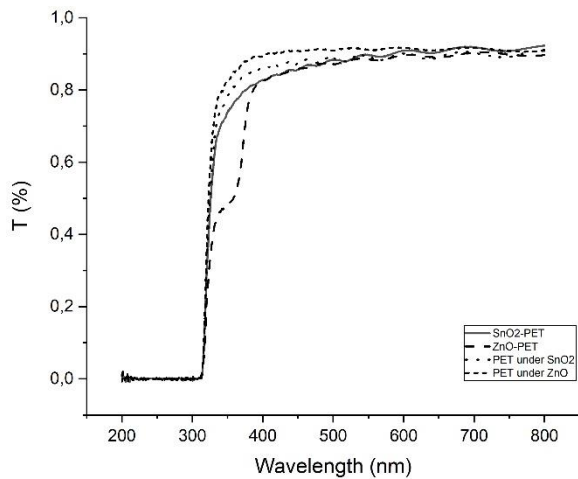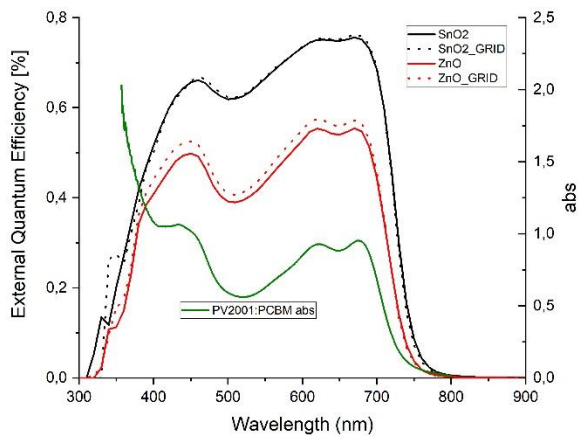
Figure 3 UV-VIS transmittance spectra of PET, PET/SnO2 and PET/ZnO

Figure 4 EQE of PV2001 with ZnO and SnO2 as ETL (with a filled (solid line) and grid (dotted line) back contact) and absorption spectra of PV2001.

Table 1 Light intensities of indoor light sources.

mW/cm^2	200 lux	400 lux	800 lux	1000 lux
FL830	0.05662	0.11167	0.22545	0.28452
LED	0.07120	0.14230	0.28471	0.35660

Table 2 Summary of photovoltaic characteristics of the PV2001:PCBM cells and modules under AM1.5.[a]

ETL	Ag	Mean I_{SC} [mA]	Mean J_{SC}/cell [mA/cm^2]	Mean V_{OC} [V]	Mean P_{max} [mW]	Mean FF [%]	Mean PCE [%]
ZnO	**Full**	3.24 ±0.5	9.83 ±1.6	0.75 ±0.0	1.13 ±0.3	46 ±3	3.4 ±0.8
	Grid	3.92 ±0.3	11.87 ±1.0	0.75 ±0.0	1.45 ±0.2	49 ±3	4.4 ±0.6
SnO₂	**Full**	3.74 ±0.4	11.34 ±1.3	0.75 ±0.0	1.20 ±0.1	43 ±2	3.6 ±0.4
	Grid	3.88 ±0.4	11.76 ±1.2	0.75 ±0.0	1.28 ±0.1	44 ±1	3.9 ±0.4
ZnO Module	**Grid**	24.40	14.35	5.97	62.41	43	4.6
SnO₂ Module	**Grid**	17.16	10.10	5.96	46.34	45	3.4

[a] The average was calculated from mesurements for 16 cells and 3 modules.

Table 3 Summary of photovoltaic characteristics of the PV2001:PCBM cells and modules under indoor light sources.[a]

ETL	Ag	light source	lux	Mean I_{SC} [μA]	Mean J_{SC}/cell [μA/cm^2]	Mean V_{OC} [V]	Mean P_{max} [μW]	Mean FF [%]	Mean PCE [%]
ZnO	Full	FL830	200	4	13.2	0.53	1.3	56	6.9
			400	9	25.9	0.56	2.4	51	6.6
			800	17	52.7	0.60	5.6	54	7.5
			1000	22	66.0	0.60	7.7	58	8.2
	Grid		200	5	15.3	0.56	1.7	60	9.0
			400	10	30.9	0.58	3.6	61	9.7
			800	20	60.7	0.60	7.4	61	10.0
			1000	25	73.6	0.61	9.3	62	9.9
	Full	LED	200	6	17.6	0.55	1.8	56	7.5
			400	10	29.8	0.57	2.7	47	5.6
			800	20	60.2	0.60	6.3	52	6.7
			1000	25	77.8	0.61	8.5	55	7.2
	Grid		200	7	20.2	0.56	2.3	61	9.7
			400	12	36.9	0.59	4.2	59	9.0
			800	23	69.5	0.61	8.6	61	9.1
			1000	30	89.9	0.62	11.5	63	9.7
SnO$_2$	Full	FL830	200	6	18.2	0.54	2.1	65	11.4
			400	12	37.8	0.57	4.7	66	12.7
			800	24	74.5	0.60	9.3	63	12.5
			1000	29	89.4	0.61	11.7	65	12.5
	Grid		200	6	19.4	0.54	2.3	66	12.3
			400	13	39.6	0.57	5.0	67	13.5
			800	26	77.6	0.60	10.0	65	13.5
			1000	31	92.9	0.61	12.2	66	12.9
	Full	LED	200	8	24.0	0.55	2.9	66	12.3
			400	15	45.5	0.57	5.6	64	11.8
			800	28	86.4	0.60	10.7	62	11.4
			1000	37	111.0	0.61	13.9	62	11.8
	Grid		200	8	24.7	0.56	3.0	67	12.9
			400	15	46.7	0.58	5.9	67	12.6
			800	29	88.2	0.60	11.5	65	12.2
			1000	37	112.8	0.61	15.0	66	12.7
ZnO Mod.	Grid	FL830	200	30	17.6	4.20	69.2	54	9.0
			400	59	35.2	4.49	150.5	57	9.9
			800	117	68.8	4.72	322.4	58	10.5
			1000	147	86.4	4.80	412.4	58	10.8
		LED	200	37	21.6	4.32	87.8	56	9.1
			400	73	43.2	4.52	192.3	58	9.9
			800	137	80.8	4.82	383.1	58	9.9
			1000	181	106.4	4.90	514.4	58	10.7
SnO$_2$ Mod.	Grid	FL830	200	38	22.4	4.33	102.8	62	13.4
			400	72	42.4	4.54	200.9	62	13.2
			800	142	84.0	4.74	409.6	61	13.4
			1000	177	104.0	4.81	513.2	60	13.4
		LED	200	44	25.6	4.40	119.0	62	12.3
			400	87	51.2	4.62	247.1	61	12.8
			800	167	98.4	4.81	490.2	61	12.7
			1000	211	124.0	4.89	628.3	61	13.0

[a] The average was calculated from mesurements for 3 cells and 3 modules.

Table 4 Series resistance and shunt resistance of modules calculated from the slope of the I-V curve under 1 sun and indoor light

ETL	Ag	light source	lux	R_S [Ω]	R_{SH} [kΩ]
ZnO	**Grid**	**AM1.5**		56.6	1.16
		FL830	200	172.5	657
			400	171.9	401
			800	164.6	231
			1000	182.8	188
		LED	200	194.4	596
			400	186.3	340
			800	188.6	196
			1000	187.0	152
SnO₂	**Grid**	**AM1.5**		45.9	1.00
		FL830	200	79.7	1326
			400	79.6	721
			800	79.0	357
			1000	81.5	290
		LED	200	80.1	1140
			400	81.4	589
			800	81.2	336
			1000	80.2	295

References

[1] R. Arai, S. Furukawa, Y. Hidaka, H. Komiyama and T. Yasuda, *ACS Appl. Mater. Interfaces,* vol. 11, p. 9259, 2019.

[2] H. K. H. Lee, J. Wu, J. Barbé, S. M. Jain, S. Wood, E. M. Speller, Z. Li, F. A. Castro, J. R. Durrant and W. C. Tsoi, *J. Mater. Chem. A,* vol. 6, p. 5618, 2018.

[3] A. E. Ostfeld and A. C. Arias, *Flex. Print. Electron.,* vol. 013001, p. 2, 2017.

[4] R. R. Søndergaard, M. Hösel and F. C. Krebs, *J. Polym. Sci. Part B: Polym. Phys. ,* vol. 51, p. 16, 2013.

[5] M. Vilkman, K.-L. Väisänen, P. Apilo, R. Po, M. Välimäki, M. Ylikunnari, A. Bernardi, T. Pernu, G. Corso, J. Seitsonen, S. Heinilehto, J. Ruokolainen and J. Hast, *ACS Appl. Energy Mater.,* vol. 1, p. 5977, 2018.

[6] L. Meng, Y. Zhang, X. Wan, C. Li, X. Zhang, Y. Wang, X. Ke, Z. Xiao, L. Ding, R. Xia, H.-L. Yip, Y. Cao and Y. Chen, *Science,* vol. 361, p. 1094, 2018.

[7] NREL, "Best Research-Cell Efficiency Chart," The National Renewable Energy Laboratory , 26 11 2019. [Online]. Available: nrel.gov/pv/cell-efficiency.html.

[8] R. Yu, H. Yao, Y. Cui, L. Hong, C. He and J. Hou, *Adv. Mater.,* vol. 31, p. 1902302, 2019.

[9] T. Yan, J. Ge, T. Lei, W. Zhang, W. Song, F. Billy, D. Zhang, S. Chen, R. Peng and Z. Ge, *J. Mater. Chem. A,* vol. 7, p. 25894, 2019.

[10] Y. Cui, Y. Wang, J. Bergqvist, H. Yao, Y. Xu, B. Gao, C. Yang, S. Zhang, O. Inganäs, F. Gao and J. Hou, *Nature Energy,* vol. 4, p. 768, 2019.

[11] H. Yin, S. Chen, S. H. Cheung, H. W. Li, Y. Xie, S. W. Tsang, X. Zhu and S. K. So, *J. Mater. Chem. C,* vol. 6, p. 9111, 2018.

[12] J. S. Goo, S.-C. Shin, Y.-J. You and J. W. Shim, *Solar Energy Mater. Solar Cells,* vol. 184, p. 31, 2018.

[13] S. Mori, T. Gotanda, Y. Nakano, M. Saito, K. Todori and M. Hosoya, *Jpn. J. Appl. Phys.,* vol. 54, p. 071602, 2015.

[14] P. Vincent, S.-C. Shin, J. S. Goo, Y.-J. You, B. Cho, S. Lee, D.-W. Lee, S. R. Kwon, K.-B. Chung, J.-J. Lee, J.-H. Bae, J. W. Shim and H. Kim, *Dyes and Pigments,* vol. 159, p. 306, 2018.

[15] S.-C. Shin, C. W. Koh, P. Vincent, J. S. Goo, J.-H. Bae, J.-J. Lee, C. Shin, H. Kim, H. Y. Woo and J. W. Shim, *Nano Energy,* vol. 58, p. 466, 2019.

[16] H. K. H. Lee, Z. Li, J. R. Durrant and W. C. Tsoi, *Appl. Phys. Lett.,* vol. 108, p. 253301, 2016.

[17] R. Steim, T. Ameri, P. Schilinsky, C. Waldauf, G. Dennler, M. Schaber and C. J. Brabec, *Solar Energy Mater. Solar Cells,* vol. 95, p. 3256, 2011.

[18] C. L. Cutting, M. Bag and D. Venkataraman, *J. Mater. Chem. C,* vol. 4, p. 10367, 2016.

[19] Y. Aoki, *Organic Electronics,* vol. 48, p. 194, 2017.

[20] P. Maisch, K. Tam, L. Lucera, H. Egelhaaf, H. Schreiber, E. Maier and C. Brabec, *Organic Electronics,* vol. 38, p. 139, 2016.

[21] T. Eggenhuisen, Y. Galagan, A. Biezemans, T. Slaats, W. Voorthuijzen, S. Kommeren, S. Shanmugam, J. Teunissen, A. Hadipour, W. Verhees, S. Veenstra, M. Coenen, J. Gilot, R. Andriessen and W. Groen, *J. Mater. Chem. A,* vol. 3, no. 14, p. 7255, 2015.

[22] M. List, T. Sarkar, P. Perkhun, J. Ackermann, C. Luo and U. Würfel, *Nature Communications,* vol. 9, p. 3631, 2018.

[23] Y.-M. Chang, C.-Y. Liao, C.-C. Lee, S.-Y. Lin, N.-W. Teng and P. H.-S. Tan, *Solar Energy Mater. Solar Cells,* vol. 202, p. 11064, 2019.

[24] S. Trost, A. Behrendt, T. Becker, A. Polywka, P. Görrn and T. Riedl, *Adv. Energy Mater.,* vol. 5, p. 1500277, 2015.

[25] G. A. dos Reis Benatto, M. Corazza, B. Roth, F. Schütte, M. Rengenstein, S. A. Gevorgyan and F. C. Krebs, *Energy Technol.,* vol. 5, p. 338, 2017.

[26] N. H. Reich, W. G. J. H. M. van Sark and W. C. Turkenburg, *Renewable Energy,* vol. 36, p. 642, 2011.

[27] M. O. Reese, S. A. Gevorgyan, M. Jorgensen, E. Bundgaard, S. R. Kurtz, D. S. Ginley, D. C. Olson, M. T. Lloyd, P. Morvillo, E. A. Katz, A. Elschner, O. Haillant, T. R. Currier, V. Shrotriya, M. Hermenau, M. Riede, K. R. Kirov, G. Trimmel, T. Rath, O. Inganäs, F. Zhang, M. Andersson, K. Tvingstedt, M. Lira-Cantu, D. Laird, C. McGuiness, S. Gowrisanker, M. Pannone, M. Xiao, J. Hauch, R. Steim, D. M. DeLongchamp, R. Rösch, H.

Hoppe, N. Espinosa, A. Urbina, G. Yaman-Uzunoglu, J.-B. Bonekamp, A. J. van Breemen, C. Girotto, E. Voroshazi and F. C. Krebs, *Solar Energy Mater. Solar Cells,* vol. 95, p. 1253, 2011.

[28] C. Waldauf, M. Morana, P. Denk, P. Schilinsky, K. Coakley, S. A. Choulis and C. J. Brabec, *Appl. Phys. Lett.,* vol. 89, p. 233517, 2006.

[29] J. Hu, Z. Wu, H. Wei, T. Song and B. Sun, *Organic Electronics,* vol. 13, p. 1171, 2012.

[30] K. Zilberberg, J. Meyer and T. Riedl, *J. Mater. Chem.,* vol. 1, p. 4796, 2013.

[31] Z. Jiang, S. Soltanian, B. Gholamkhass, A. Aljaafari and P. Servati, *RSC Adv.,* vol. 8, p. 36542, 2018.

[32] S. Huang, Y. Tang, A. Yu, Y. Wang, S. Shen, B. Kang, S. R. P. Silva and G. Lu, *Org. Electronics,* vol. 62, p. 373, 2018.

[33] Z. Yang, T. Zhang, J. Li, W. Xue, C. Han, Y. Cheng, L. Qian, W. Cao, Y. Yang and S. Chen, *Scientific Reports,* vol. 7, p. 9571, 2017.

[34] N. Wu, Q. Luo, S. Bao, J. Lin, Y. Li and C. Ma, *Solar Energy Mater. Solar Cells,* vol. 141, p. 248, 2015.

[35] Y. Jiang, L. Sun, F. Jiang, C. Xie, L. Hu, X. Dong, F. Qin, T. Liu, L. Hu, X. Jiang and Y. Zhou, *Mater. Horiz.,* vol. 6, p. 1438, 2019.

[36] J. Kim, G. Kim, Y. Choi, J. Lee, S. Heum Park and K. Lee, *J. Appl. Phys.,* vol. 111, p. 114511, 2012.

[37] W. Ke, G. Fang, Q. Liu, L. Xiong, P. Qin, H. Tao, J. Wang, H. Lei, B. Li, J. Wan, G. Yang and Y. Yan, *J. Am. Chem. Soc.,* vol. 137, p. 6730, 2015.

[38] E. H. Anaraki, A. Kermanpur, L. Steier, K. Domanski, T. Matsui, W. Tress, M. Saliba, A. Abate, M. Grätzel, A. Hagfeldt and J.-P. Correa-Baena, *Energy Environ. Sci.,* vol. 9, p. 3128, 2016.

[39] Z. Zhu, Y. Bai, X. Liu, C.-C. Chueh, S. Yang and A. K.-Y. Jen, *Adv. Mater.,* vol. 28, p. 6478, 2016.

[40] Q. Jiang, L. Zhang, H. Wang, X. Yang, J. Meng, H. Liu, Z. Yin, J. Wu, X. Zhang and J. You, *Nat. Energy,* vol. 2, p. 16177, 2016.

[41] B. Bob, T.-S. Song, C.-C. Chen, Z. Xu and Y. Yang, *Chem. Mater.,* vol. 25, p. 4725, 2013.

[42] V.-H. Tran, R. B. Ambade, S. B. Ambade, S.-H. Lee and I.-H. Lee, *Appl. Mater. Interfaces,* vol. 9, p. 1645, 2017.

[43] T. Bu, J. Li, F. Zheng, W. Chen, X. Wen, Z. Ku, Y. Peng, J. Zhong, Y.-B. Cheng and F. Huang, *Nature Commun.,* vol. 9, p. 4609, 2018.

[44] N. Grossiord, J. M. Kroon, R. Andriessen and P. W. Blom, *Org. Electronics,* vol. 13, p. 432, 2012.

[45] C. M. Proctor and T.-Q. Nguyen, *Appl. Phys. Lett.,* vol. 106, p. 083301, 2015.

[46] M. Tavakoli, H. Dastjerdi, J. Zhao, K. Shulenberger, C. Carbonera, R. Po, A. Cominetti, G. Bianchi, N. Klein, M. Bawendi, S. Gradecak and J. Kong, *Small,* vol. 15, p. 1900508, 2019.

[47] Yrjänä, 2014.

[48] H. Yin, J. K. W. Ho, S. H. Cheung, R. J. Yan, K. L. Chiu, X. Hao and S. K. So, *J. Mater. Chem. A,* vol. 6, p. 8579, 2018.

[49] Z. Xiao, X. Jia and L. Ding, *Science Bulletin,* vol. 62, p. 1562, 2017.

[50] J. Hou, O. Inganäs, R. H. Friend and F. Gao, *Nature Materials,* vol. 17, p. 119, 2018.